ADSORPTION OF 2-THIOBARBITURIC ACID AT THE ELECTROCHEMICAL INTERFACE: CONTRASTED BEHAVIOURS ON MERCURY AND GOLD

Thomas DONEUX[1], Mustapha EL ACHAB[2] and Claudine BUESS-HERMAN[3,*]

Chimie Analytique et Chimie des Interfaces, Faculté des Sciences, Université Libre de Bruxelles, Boulevard du Triomphe, 2, CPI 255, 1050 Bruxelles, Belgium;
e-mail: [1] tdoneux@ulb.ac.be, [2] labcb@ulb.ac.be, [3] cbuess@ulb.ac.be

Received October 1, 2009
Accepted October 20, 2009
Published online December 17, 2009

Dedicated to the 50th anniversary of rewarding the Nobel prize to Professor Jaroslav Heyrovský for the discovery of polarography.

The adsorption of 2-thiobarbituric acid (TBA) from acid solutions (pH ~1) has been investigated at the Au(111) single crystal electrode and at the dropping mercury electrode. In contrast to the gold electrode where the adsorption is driven by the strong interaction between Au and the S atom, the TBA adsorption at the mercury electrode is more contrasted and distinct features such as capacitance pits are observed in the capacitance–potential curves. The kinetics of phase transformation were investigated by the potential step technique. The formation of films B and C prevailing in two distinct capacity pit regions is controlled by a nucleation and growth mechanism. Ordering of film A observed at the positive end of the potential region is also evidenced on the basis of the charge transients associated with its formation from film B or C. The two successive sigmoidal parts in the charge transient obtained at small overpotentials for the transformation of C to A is explained by the presence of an intermediate metastable film.

Keywords: 2-Thiobarbituric acid; Polarography; Gold electrode; Phase transition; Nucleation and growth; Electrochemistry.

Fundamental work dealing with the adsorption of organic or biomolecules at the metal|solution interface has, during several decades, essentially been performed at mercury electrodes[1–4]. The mercury electrode has great advantages over solid electrodes including even single crystal electrodes since its surface is easily renewed, smooth and energetically uniform. It is therefore not surprising that the mercury electrode is presently still used in research area such as the study of biomimetic membranes[5,6] or the electrochemistry

© 2009 Institute of Organic Chemistry and Biochemistry
doi:10.1135/cccc2009515

in ionic liquids[7] where a drastic control of the electrified interface is required in order to be able reproduce and to interpret the experimental data.

Besides the mercury electrode, the gold electrode and more specifically gold single crystals have been extensively used to examine the adsorption of organic molecules[8–10]. In particular the possibility to spontaneously form self-assembled monolayer (SAM) of thiols on gold through a chemisorption process has stimulated a lot of work regarding the electrochemical stability and properties of the SAMs[11,12]. In addition to alkanethiols, heterocyclic thiols also received some attention due to the high conductivity and stability of the SAMs that they form on gold. Among these, the interaction of gold with 2-thiobarbituric acid (TBA) has been considered in the construction of supramolecular entities by combining aurophilicity and hydrogen bonding[13], the synthesis of gold nanoparticles[14] and the formation of artificial chemoreceptors[15]. Very recently Méndez et al.[16] have reported on the electron-transfer properties of a polycrystalline gold electrode modified by a SAM of TBA.

The use of mercury instead of gold allows us to explore a potential range that is extended to more negative values due to the large overvoltage for hydrogen evolution on mercury but is limited at positive potentials by the oxidation of mercury. As a result, the adsorption data that may be obtained by resorting to gold and to mercury electrodes lead to a more complete description of the adsorption behaviour of surfactants at electrified interfaces. Significant differences in the adsorption of azabenzenes have been observed by changing the metal electrode from mercury to gold. The coordination of the azabenzenes such as pyridine[17] or isoquinoline[18] to the gold surface leads to a weak chemisorption and in the vertical position the molecules are oriented with the nitrogen toward the metal and with the hydrocarbon part toward the solution. This vertical orientation is opposite to that observed at the mercury electrode where flat orientation prevails at small negative potentials while at large negative potentials reorientation of the molecules takes place orienting the dipole in the field with the nitrogen facing the solution. The use of gold and mercury is therefore also expected to yield a complementary adsorption behaviour for TBA as a function of the applied potential.

In the early seventies, the electrochemical behaviour of some sulfur-containing drugs at the mercury electrode has been intensively studied for analytical purposes as well as for the establishment of a relationship between physicochemical properties and pharmacological activity. In this respect several groups have investigated the polarographic and cathodic stripping behaviour of thiobarbituric acid and derivatives[19–24]. Several

waves have been detected depending on the pH of the solution and the concentration of TBA. An oxidation wave associated to the formation of an organomercurial salt as well as adsorption phenomena were reported for TBA. The first attempt to study the adsorption behaviour of TBA at the mercury|solution interface has been carried out by Kamal[25]. On the basis of phase-sensitive AC voltammograms obtained at the hanging mercury drop electrode in a Britton–Robinson buffer (at pH 3.2, 7.3 and 9.35), two adsorption states were identified for TBA. Besides a dilute film, a capacitance pit reflecting the association of TBA molecules by intermolecular attractive forces is evidenced at sufficiently high concentrations. While desorption is observed at negative potentials in alkaline solutions, sharp peaks are detected at the positively charged electrode surface due to the electroreduction of the Hg(II) ion of the $Hg(RS^-)_2$ formed between RS^- species and the mercury surface.

The present paper is aimed at showing the multiplicity of adsorbed states presented by 2-thiobarbituric acid at the mercury electrode in contrast to its behaviour at a gold electrode, where chemisorption prevails. Kinetic information obtained from chronocoulometric measurements will complete the capacitance and charge characteristics of the TBA condensed adsorption states. TBA is a mercaptopyrimidine derivative presenting many tautomeric forms[26,27] affecting the amplitude of its dipole moment. The predominant tautomer is presented in Scheme 1A. TBA is also involved in acid-base equilibria with associated pK_a values of 2.25 and 10.72 (ref.[19]). In this work, all measurements are performed at pH ≈ 1 in order to study the adsorption of only one defined neutral species. It has been established that co-adsorption of the electrolyte anions affects the formation of condensed films, for instance in the case of thiourea[28]. Therefore, co-adsorption was avoided in the present work by using respectively perchloric acid and sulfuric for the measurements at the gold and mercury electrode.

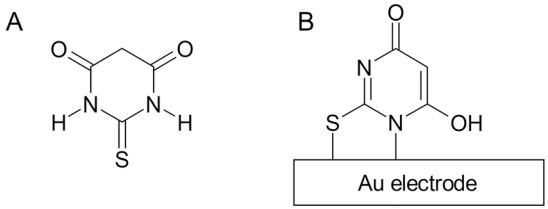

SCHEME 1
A Structure of the 2-thiobarbituric acid molecule (predominant tautomer in the solid state). B Interaction of TBA with gold surfaces, as proposed in ref.[27]

EXPERIMENTAL

Solutions

The solutions made from Milli-Q water were prepared by weighing and dissolving a known amount of 2-thiobarbituric acid (Fluka, purity 99%+ grade) in the supporting electrolyte. Perchloric acid (Merck Suprapur®) and sulfuric acid (Merck Suprapur®) were used as electrolytes. All solutions were purged with highly purified nitrogen before the experiments and nitrogen was passed over the top of the solution during the measurements.

The whole water-jacketed electrochemical cell was kept at constant temperature (±0.1 °C) by a Julabo F10-VC thermostat-cryostat.

Electrodes

The working electrodes were a dropping mercury electrode (DME) and a home-made gold (111) single-crystal electrode. The single crystal was grown, oriented and polished in the lab according to the procedure developed by Hamelin[29]. Using the hanging meniscus technique, only the (111) face of the electrode was in contact with the electrolyte. The counter electrode consisted of a large area gold wire. The purity of the gold (Johnson Matthey) used for the working and counter electrode was 99.9985%. The reference electrode was a KCl saturated calomel electrode connected to the cell through a salt bridge. All the potentials given in this paper refer to the saturated calomel electrode (SCE).

Prior to each experiment, the gold working electrode was annealed in a gas-oxygen flame, cooled down a few seconds in air and then quickly quenched in pure water. This treatment provides us a clean and well-ordered reconstructed surface.

Equipment

Electrochemical experiments at the gold|electrolyte interface were performed in a three electrode cell connected to an Autolab PGSTAT 20 (Eco Chemie) equipped with a Scangen.

Tensammetric data, charge density potential curves and chronocoulometric data performed at the DME were obtained as reported previously[30].

RESULTS AND DISCUSSION

Adsorption at the Au(111) Electrode

At the gold|electrolyte interface, 2-thiobarbituric acid presents the adsorption features typical of the thiol compounds. A self-assembled monolayer can be formed by simple immersion of the (111) face of the gold electrode in a 10^{-3} M aqueous solution of TBA. After 15 min of immersion at 25 °C, the electrode was thoroughly rinsed with pure water, dried and transferred in the electrochemical cell containing only pure electrolyte. The modified electrode remains stable, even after 15 h, when it is placed in contact with the TBA free electrolyte solution in the absence of polarization.

Under polarization, the SAM formed by the immersion procedure undergoes significant modifications. The voltammograms recorded in the so-called double layer region of the gold electrode are significantly affected upon cycling, as shown in Fig. 1.

When scanning in the negative direction, a broad peak is observed, before hydrogen evolution takes place. In the positive scan, an anodic peak is detected and upon cycling the intensities of the cathodic and anodic peaks decrease with the number of scans. This behaviour is typical of a "reductive desorption" occurring to self-assembled monolayers of thiols on gold (e.g. refs[31,32]). When the potential is scanned in the negative direction, a reduction process occurs, breaking the chemical bond between the gold and sulfur atoms. The organic molecules may then desorbed from the surface and diffuse into the solution. When the scan is reversed, a certain amount of molecule may, depending on the elapsed time, be readsorbed following a reverse reaction.

A similar curve is observed when TBA is present in solution although at potentials more positive than 0.5 V the back scan leads to a higher anodic current indicating that oxidation of non-adsorbed molecules takes place.

The analysis of the CV curves in terms of the charge involved in the reduction process provides an estimate of the surface excess of the surfactant. After correction for capacitive contribution the charge density for the reductive desorption amounts to 35 ± 3 $\mu C/cm^2$ which leads to a surface

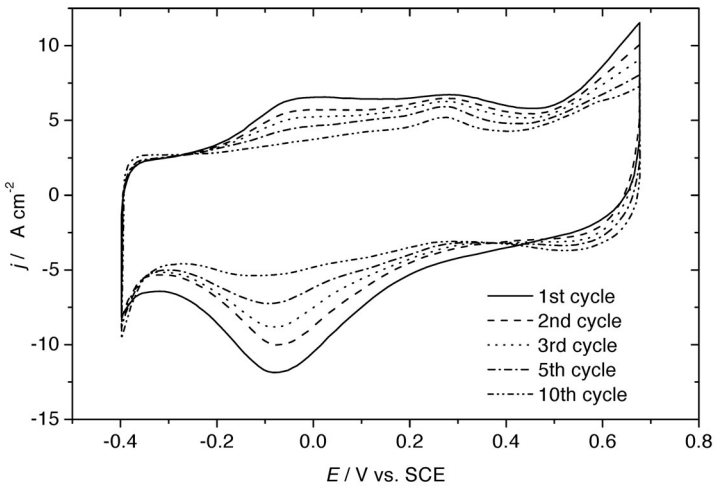

FIG. 1
Consecutive cyclic voltammograms of a SAM of 2-thiobarbituric acid formed on Au(111), recorded in 0.1 M $HClO_4$ at a scan rate of 50 mV/s

excess of 3.6×10^{-10} mol/cm^2 for a one electron process. From this value, one can calculate a projected area per molecule of 46 Å^2. On the basis of the crystallographic parameters of solid TBA [33], the mean molecular area is found to be 57 Å^2 for a "flat" oriented molecule and 30 Å^2 for a "vertically" oriented molecule with the C_2-axis perpendicular to the electrode surface. The experimental value of 46 Å^2 provides evidence that TBA molecules are not lying flat on the surface as was proposed by Mirsky et al.[15] but rather adopt a vertical orientation. The orientation of the TBA molecules differs, however, from the on-top configuration with the C_2-axis perpendicular to the electrode surface and is more in agreement with the on-top configuration (Scheme 1B) proposed by Méndez et al.[16] where the chemisorption of TBA involves the S atom but also a N atom.

Adsorption at the Mercury Electrode

The adsorption behaviour of TBA at the dropping mercury electrode was investigated by measuring the interfacial capacity in presence of TBA dissolved in 0.1 M sulfuric acid. The capacitance–potential curves recorded at a 4 s mercury drop for 1 mM 2-thiobarbituric acid at different temperatures are shown in Fig. 2. The interfacial behaviour of TBA at the mercury electrode differs markedly from its adsorption at the gold electrode since a di-

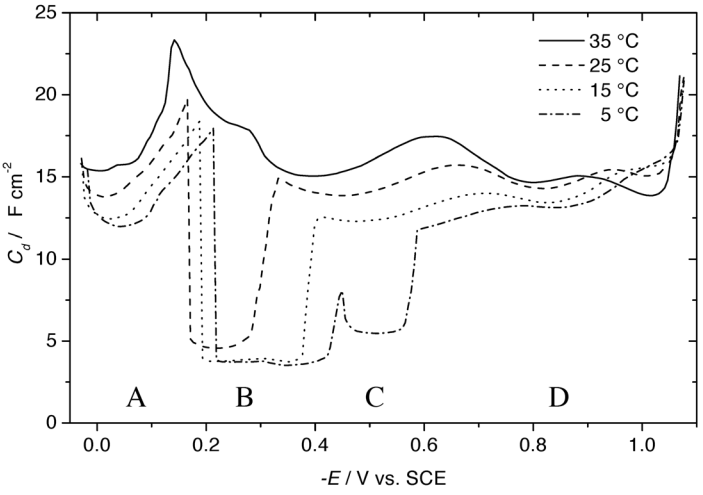

FIG. 2
Capacitance–potential curves of 1 mM 2-thiobarbituric acid in 0.1 M H_2SO_4 measured at the DME at different temperatures, as indicated in the legend. f = 117 Hz. A, B, C and D refer to various films of TBA (see the text for details)

versity of interfacial states is evidenced by various distinct regions in the capacitance curve.

The domain in which TBA film progressively changes with potential (zone D) is limited at negative potentials by the occurrence of proton reduction. Experiments performed in neutral solutions have clearly shown that TBA desorbs at very negative potentials[25]. At positive potentials (region A) the adsorption behaviour is complicated by the onset of charge transfer phenomena involving the mercury and TBA. Like other sulfur-containing molecules, TBA exhibits anodic polarographic waves corresponding to the formation of mercury compounds[22]. The overall charge transfer reaction taking place at positive potentials is analogous to the reaction leading to the chemisorption of thiols on gold.

At temperature lower than 35 °C, TBA adsorption presents some features which differ markedly from the behaviour observed at a gold surface. The use of mercury instead of gold allows us to explore the behaviour of TBA at potentials where chemisorption is no longer prevailing.

It is well established that highly densely packed physisorbed films are detected in the C_d–E curves by the presence of small capacities independent of potential, temperature and concentration[9,10,34–38]. Moreover, sharp variations associated with the existence of two-dimensional phase transitions delimit the domain of prevalence of the condensed films. Figure 2 clearly shows the presence of distinct superficial states among which films B and C are characterized by two capacitance pits. The presence of a capacitance pit is a typical feature indicating the existence of a condensed or ordered monolayer. As expected from interfacial thermodynamics, a capacitance pit is associated to the presence of steps in the corresponding charge density–potential curve. Figure 3, showing the charge curve recorded for 1 mM TBA at 15 °C, reveals that two charge steps encompass the domain of existence of film B. The point of zero charge (PZC) of film B evaluated by extrapolating the charge potential curve characteristic of film B amounts to –0.92 V. According to the Rideal equation, the shift of the PZC (compared to the PZC observed in the absence of the surfactant) indicates that adsorbed molecules in film B present a dipole contribution perpendicular to the surface. Moreover, since the PZC is displaced to more negative value, the molecules present the negative end of the dipole (sulfur atom) directed to the electrode surface. A quantitative analysis cannot be performed, due to the difficulty to assess the tautomeric form of the adsorbed molecules and the corresponding dipole moment.

Examination of the charge–potential curve measured at 5 °C clearly indicates that a smaller negative shift of the PZC is observed for film C while

the PZC of film B is unchanged at lower temperature. This result, analysed in terms of the Rideal equation, suggests that film C is less densely packed than film B since the dipolar component is expected to be larger at more negative potentials. This is confirmed by capacity and charge measurements performed in the presence of various TBA concentrations that show that film B extends its stability region over film C at higher TBA bulk concentrations.

The domain of stability of a well-ordered state is also expected to extend with a decrease in temperature[38]. Film B extends its stability range even when film C is also detected. Since the discontinuities observed in the tensammetric curves are subject to kinetic limitations, the present trend has also been confirmed by resorting to the double step procedure to properly measure the equilibrium transition potentials[39].

The condensed nature of film B is proven also by its kinetics of formation that have been examined by recording charge transients consecutive to a potential step across the transition observed for 1 mM TBA at 15 °C. All transients present a sigmoidal shape characteristic of a nucleation and growth mechanism. Of particular interest is the formation of film B from

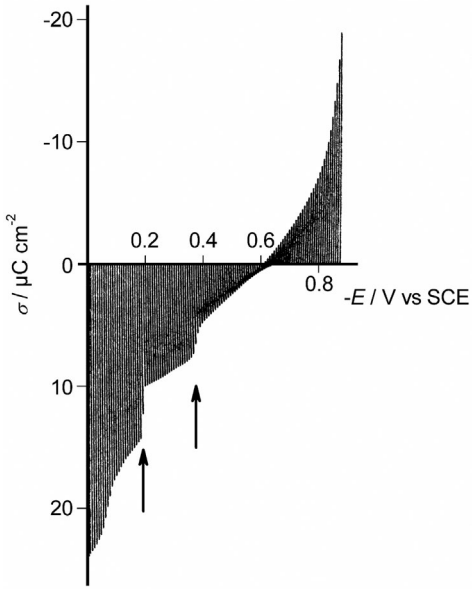

FIG. 3
Charge density–potential curve measured at the DME in a solution of 1 mM 2-thiobarbituric acid in 0.1 M H_2SO_4 at 15 °C. The arrows delimit the stability domain of film B

an initial potential located in region A. Figure 4 shows typical charge transients obtained by stepping the potential from E_i = –170 mV (in region A) to various final potentials located within the capacitance pit.

A fast initial rise of the charge caused by the sudden dielectric polarization of the existing film ($\Delta\sigma_p$) is followed by an S-shaped relaxation transient characteristic of a nucleation and growth mechanism. When the final potential is made more negative the shorter transients indicate faster film formation.

Since the extent of coverage by the new phase can be directly related to the charge density, the fraction of the surface covered by the condensed phase θ at any time is obtained by

$$\theta = (\Delta\sigma(t) - \Delta\sigma_p)/\Delta\sigma_t$$

where $\Delta\sigma_p$ is the charge needed to form the metastable state and $\Delta\sigma_t$ is the charge of the transition.

The transients have been analysed according to the following relation

$$\ln[-\ln(1 - \theta)] = m \ln t + B$$

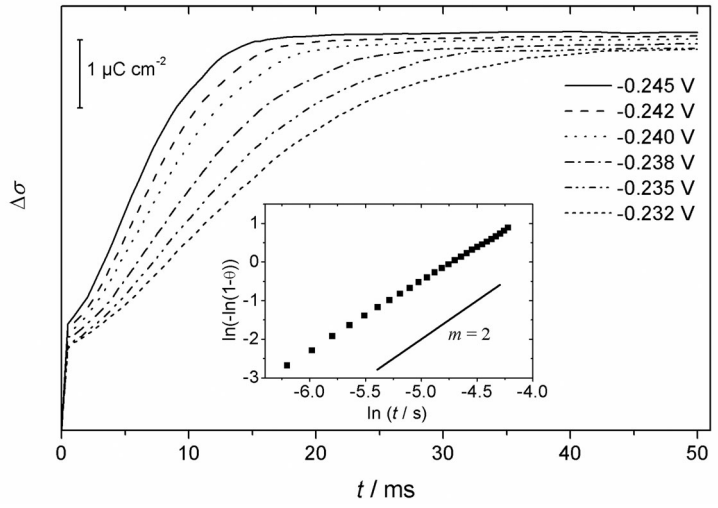

FIG. 4

Typical charge transients obtained at 15 °C by stepping the potential from E_i = –0.170 V (in region A) to various final potentials located within the capacitance pit (as indicated in the legend). Inset: Avrami plot calculated for the final potential E_f = –0.242 V. A solid line with slope m = 2 is shown for comparison

which is the linearized Avrami equation. Good straight lines are obtained in the Avrami plots as illustrated for a transient in the inset of Fig. 4. The slopes are close to 2 which is associated to a two-dimensional instantaneous nucleation and growth. When the final potential is less negative and the film relaxation is much slower one observes however a more complex response. Two successive kinetic steps can be observed (Fig. 5) since the sigmoidal transient is clearly preceded at short times by a monotonic charge variation.

Monotonic transients usually reflect a process controlled by diffusion or adsorption-desorption kinetics. The analysis of the first part of the charge–time response excludes a diffusion control. Moreover a straight line is obtained by plotting $\ln(1 - \theta)$ as a function of time (inset A) indicating a change in the monolayer prevailing at the initial potential. Although the analysis of the sigmoidal part is complicated by the first process taking place, a slope close to 2 is observed in the Avrami plot (inset B) so that one may consider that the formation of film B proceeds through a reorganisation of the initial film A which induces the formation of nuclei from which the transformation proceeds. These data indicate that film A is not a dilute physisorbed monolayer but rather a more dense monolayer, probably re-

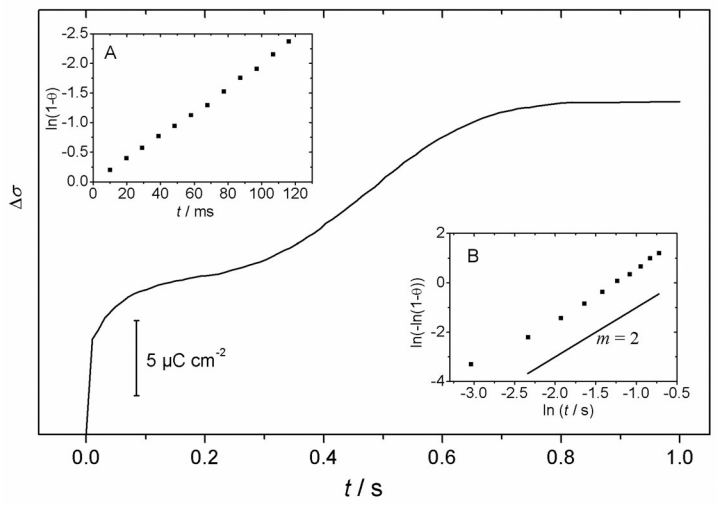

FIG. 5

Charge transient obtained at 15 °C by stepping the potential from E_i = –0.170 V (in region A) to a final potential E_f = –0.212 V (in region B). Insets present the analyses of the first (inset A) and second (inset B) parts of the transient. A solid line with slope m = 2 is shown for comparison

sulting from the chemical interaction between mercury and the sulfur compound taking place at less negative potentials. Confirmation of the dense character of the monolayer prevailing at –170 mV (region A) has been obtained from the analysis of charge transients initiated from a condensed state. At 5 °C transients were recorded by stepping the potential from –450 mV (film C) to final potentials located in region A and B. Figure 6 presents typical transients obtained at large overpotentials located in zone A.

The analysis shows that the kinetics follow a progressive nucleation and growth mechanism characterized by an Avrami slope of 3. By stepping to a potential located in region A but very close to the transition potential, an unusual curve is obtained since the transient splits into two distinct sigmoidal parts as shown in Fig. 7.

Analysis of the first part of the transient according to the Avrami formalism leads to a slope between 2 and 3 as shown in Fig. 7. No attempts have been made to fit the data to a more complex nucleation and growth mechanism involving an exponential law for nucleation or a diffusion control for the growth step nor to interpret the second part of the transient since it is very hazardous to deconvolute the two parts of the overall relaxation transient. The two successive transients provide, however, clear evidence for the

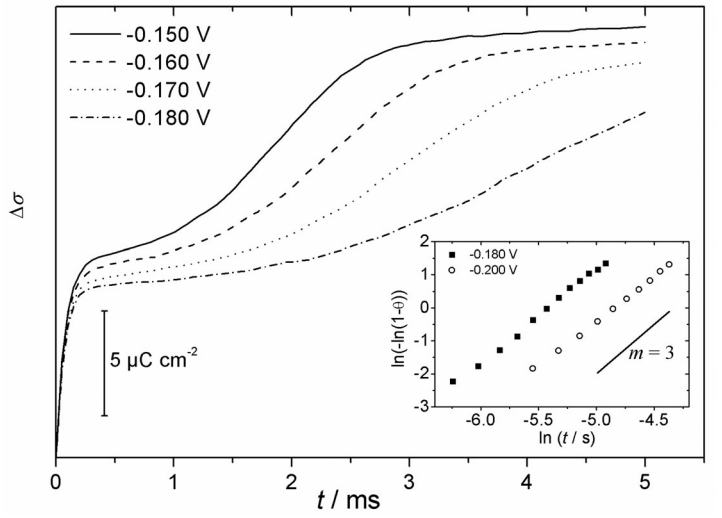

FIG. 6

Charge transients recorded at 5 °C by stepping the potential from E_i = –0.450 V (film C) to final potentials E_f located in region A, as indicated in the legend. The inset shows some corresponding Avrami plots. A solid line with slope m = 3 is shown for comparison

existence of distinct metastable states from which the formation of film A takes place. Consecutive kinetic processes have been reported earlier for thiourea[40] and other systems[39–41] but in most case a monotonous part was preceding a sigmoidal curve.

The kinetic data obtained in Fig. 7 reveal that the successive transients associated to the formation of film A involve the passage from C to B followed by the transformation of film B to film A. This is supported by the relative electrocapillary curves (Fig. 8) of the various films, constructed from the capacitance and charge values characteristic of the stable and metastable states and from the PZC (estimated from the charge density–potential curves) of the various films. At potentials more positive than the transition potential detected at –212 mV film B is a metastable state.

Depending on the respective kinetics of transformation of C to B and B to A, a single or more complex response can be detected. Indeed the formation of film B from C is rather slow at small overpotentials referred to –212 mV leading to two distinct portions in the transient while at larger overpotentials, where the supersaturation is larger, only a single sigmoidal curve is observed.

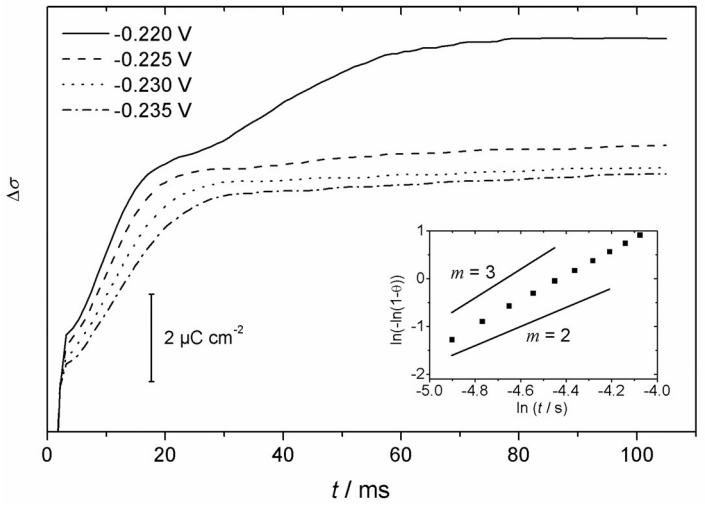

FIG. 7

Charge transients recorded at 5 °C by stepping the potential from E_i = –0.450 V (film C) to final potentials E_f located in regions B and A, as indicated in the legend. Inset: Avrami plot corresponding to the first part of the transient at E_f = –0.220 V. Solid lines with slope m = 2 and 3 are shown for comparison

CONCLUSIONS

The 2-thiobarbituric adsorption data obtained by resorting to gold and mercury electrodes show distinct differences but also similitudes. In both cases, the interaction of the S atom with the electrode surface has to be considered. This interaction is much stronger for the gold surface so that chemisorption dominates and no other additional adsorbed film is detected as a function of potential. Reductive desorption starts at positive potentials and extends to negative values so that no double layer region can be detected before the hydrogen evolution takes place. Using a mercury electrode, the study of the adsorption behaviour for TBA as a function of the applied potential can be extended to more negative potentials. While at positive potentials a chemical interaction between Hg and TBA exists, at negative potentials TBA is no longer bound to the electrode surface and different adsorption states may be triggered by changing the electric field before the onset of the proton reduction. All adsorption states on mercury involve the TBA molecules oriented with the S atom toward the electrode surface since negative shifts of the PZC are associated to the different films. At the

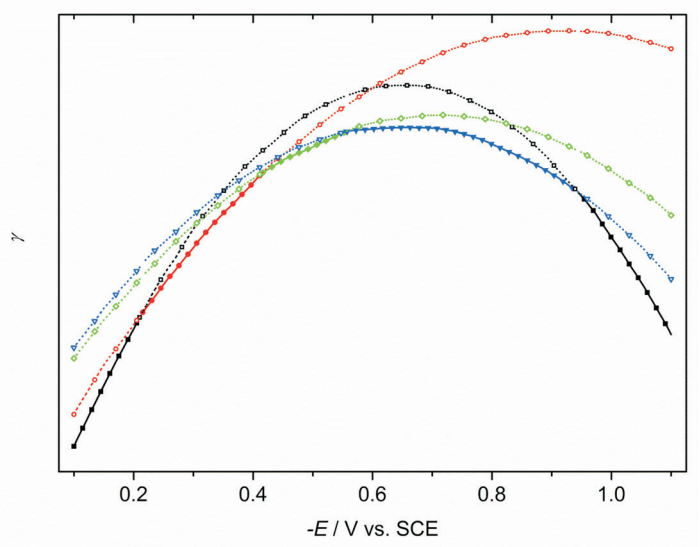

FIG. 8
Relative electrocapillary curves of films A (black squares), B (red circles), C (green diamonds) and D (blue triangles), calculated for 1 mM 2-thiobarbituric acid in 0.1 M H_2SO_4 at 5 °C. Solid lines and full symbols correspond to the equilibrium state, while the dotted lines with open symbols represent metastable states

mercury electrode, three distinct films may be considered as ordered monolayers. While films B and C are clearly encompassed by sharp phase transitions characteristic of the presence of condensed monolayers, film A whose domain of stability is only clearly limited at the negative potential side is, however, formed by a nucleation and growth mechanism, which strongly suggests the existence of ordering in the layer.

Th. Doneux (Postdoctoral researcher) gratefully acknowledges the financial support from the Fonds National de la Recherche Scientifique (F.R.S.-FNRS). This research was supported by the Belgian National Science Foundation (F.R.F.C. project).

REFERENCES

1. Damaskin B. B., Petrii O. A., Batrakov V. V.: *Adsorption of Organic Compounds on Electrodes*. Plenum Press, New York–London 1971.
2. Damaskin B. B., Kazarinov V. E. in: *Comprehensive Treatise of Electrochemistry* (J. O'M. Bockris, B. E. Conway and E. Yeager, Eds), Vol. 1. Plenum Press, New York–London 1980.
3. Damaskin B. B., Petrii O. A. in: *Encyclopedia of Electrochemistry* (E. Gileadi and M. Urbakh, Eds), Vol. 1, p. 323. Wiley–VCH, Weinheim 2002.
4. Palecek E., Scheller F., Wang J. (Eds): *Electrochemistry of Nucleic Acids and Proteins. Towards Sensors for Genomics and Proteomics*. Elsevier, Amsterdam 2005.
5. Bizzotto D., Yang Y., Shepherd J. L., Stoodley R., Agak J., Stauffer V., Lathuilliere M., Akhtar A. S., Chung E.: *J. Electroanal. Chem.* **2004**, *574*, 167.
6. Guidelli R., Aloisi G., Becucci L., Dolfi A., Moncelli M. R., Buoninsegui F. T.: *J. Electroanal. Chem.* **2001**, *504*, 1.
7. Silva F., Gomes C., Figueiredo M., Costa R., Martins A., Pereira C. M.: *J. Electroanal. Chem.* **2008**, *622*, 153.
8. Lipkowki J., Stolberg L. in: *Adsorption of Molecules at Metal Electrodes* (J. Lipkowski and Ph. N. Ross, Eds), p. 171. VCH Publishers, Weinheim 1992.
9. Bare S., Van Krieken M., Buess-Herman C., Hamelin A.: *J. Electroanal. Chem.* **1998**, *445*, 7.
10. Wandlowski Th. in: *Encyclopedia of Electrochemistry* (E. Gileadi and M. Urbakh, Eds), Vol. 1, p. 383. Wiley–VCH, Weinheim 2002.
11. Ulman A.: *Chem. Rev.* **1996**, *96*, 1533.
12. Love J. C., Estroff L. A., Kriebel J. K., Nuzzo R. G., Whitesides G. M.: *Chem Rev.* **2005**, *105*, 1103.
13. Hunks W. J., Jennings M. C., Puddephatt R. J.: *Inorg. Chem.* **2002**, *41*, 4590.
14. Peng Z., Walther Th., Kleinermanns K.: *Langmuir* **2005**, *21*, 4249.
15. Mirsky V. M., Hirsch Th., Piletsky S. A., Wolfbeis O. S.: *Angew. Chem. Int. Ed.* **1999**, *38*, 1108.
16. Méndez E., Wörner M., Lages C., Cerdá M. F.: *Langmuir* **2008**, *24*, 5146.
17. Stolberg L., Richer J., Lipkowski J.: *J. Electroanal. Chem.* **1986**, *207*, 213.
18. Yang D.-F., Lipkowski J.: *Langmuir* **1994**, *10*, 2647.
19. Smyth W. F., Svelha G., Zuman P.: *Anal. Chim. Acta* **1970**, *51*, 489.
20. Smyth W. F., Svelha G., Zuman P.: *Anal. Chim. Acta* **1970**, *52*, 129.
21. Smyth W. F., Zuman P., Svelha G.: *Anal. Chim. Acta* **1970**, *51*, 489.

22. Mairesse-Ducarmois C. A., Patriarche G. J., Vandenbalck J. L.: *Anal. Chim. Acta* **1975**, *79*, 69.
23. Osman Solak A., Temizer A.: *J. Electroanal. Chem.* **1983**, *151*, 101.
24. Ivaska A., Vaneesorn Y., Davidson I. E., Smyth W. F.: *Anal. Chim. Acta* **1980**, *121*, 51.
25. Kamal M.: *Bioelectrochem. Bioenerg.* **1991**, *26*, 359.
26. Millefiori S., Millefiori A.: *J. Heterocycl. Chem.* **1989**, *26*, 639.
27. Méndez E., Cerdá M. F., Gancheff J. S., Torres J., Kremer C., Castiglioni J., Kieninger M., Ventura O. N.: *J. Phys. Chem. C* **2007**, *111*, 3369.
28. Buess-Herman C., Gierst L., Gonze M., Silva F.: *J. Electroanal. Chem.* **1987**, *226*, 267.
29. Hamelin A. in: *Trends in Interfacial Electrochemistry* (A. F. Silva, Ed.). Reidel, Dordrecht 1986.
30. Buess-Herman C., Gierst L., Vanlaethem-Meurée N.: *J. Electroanal. Chem.* **1986**, *123*, 1.
31. Calvente J. J., Kovacova Z., Sanchez M. D., Andreu R., Fawcett W. R.: *Langmuir* **1996**, *12*, 5696.
32. Sumi T., Uosaki K.: *J. Phys. Chem. B* **2004**, *108*, 6422.
33. Calas M.-R., Martinez J.: *C. R. Acad. Sci. Paris, Ser. C* **1967**, 631.
34. Vetterl V.: *Collect. Czech. Chem. Commun.* **1966**, *31*, 2105.
35. Buess-Herman in: *Trends in Interfacial Electrochemistry* (A. F. Silva, Ed.), p. 205. Reidel, Dordrecht 1986.
36. de Levie R.: *Chem. Rev.* **1988**, *88*, 599.
37. Buess-Herman C., Baré S., Poelman M., Van Krieken M. in: *Interfacial Electrochemistry* (A. Wieckowski, Ed.), p. 427. M. Dekker, New York 1999.
38. Buess-Herman C., Franck C., Gierst L.: *Electrochim. Acta* **1986**, *31*, 965.
39. Skompska M., Buess-Herman C.: *J. Chem. Soc., Faraday Trans.* **1996**, *92*, 3940.
40. Wandlowski T., de Levie R.: *J. Electroanal. Chem.* **1993**, *345*, 413.
41. Scharfe M., Buess-Herman C.: *J. Electroanal. Chem.* **1994**, *366*, 303.